Supplement of Atmos. Chem. Phys., 19, 14365–14385, 2019
https://doi.org/10.5194/acp-19-14365-2019-supplement

Atmospheric Chemistry and Physics
Open Access
EGU

Supplement of

Importance of dry deposition parameterization choice in global simulations of surface ozone

Anthony Y. H. Wong et al.

Correspondence to: Jeffrey A. Geddes (jgeddes@bu.edu)

1. Mathematical analysis for sensitivity of O_3 to $\Delta v_d/v_d$:

Assume that ΔO_3 is due to changes in dry deposition flux (with proportionality constant k_d) and other first-order processes (e.g. NO titration, loss to HO_2 and OH, having total reaction rate k_c):

$$dO_3 = d(-k_c O_3 - k_d v_d O_3) \ (S1)$$

Here, k_c and k_d (which are related to meteorology and concentration of other relevant chemical species), are assumed to be relatively constant, so that that the perturbation in v_d does not trigger significant non-linearity. Expanding the differential and rearranging the terms yields:

$$\frac{dO_3}{O_3} = \frac{-k_d\, dv_d}{1 + k_c + k_d} \ (S2)$$

Integrating S2 between perturbed ($O_3 + \Delta O_3$, $v + \Delta v_d$) and unperturbed (O_3 and v_d) values yields:

$$\ln\left(1 + \frac{\Delta O_3}{O_3}\right) = -\ln\left(1 + \frac{k_d \Delta v_d}{1 + k_c + k_d v_d}\right) \ (S3)$$

Since ΔO_3 is small compared to $O_{3,0}$, first-order expansion is valid. When Δv_d is small enough relative to v_d for first-order approximation, Taylor's expansion of S4 yield:

$$\frac{\Delta O_3}{O_3} = -\frac{k_d}{1 + k_c + k_d v_d} \Delta v_d \ (S4)$$

S5 can be rearranged to yield:

$$\Delta O_3 = -\frac{k_d v_d O_3}{1 + k_c + k_d v_d} \frac{\Delta v_d}{v_d} = \beta \frac{\Delta v_d}{v_d}, where\ \beta = -\frac{k_d v_d O_3}{1 + k_c + k_d v_d} < 0 \ (S5)$$

This shows that when the $\Delta v_d/v_d$ is small enough ($\ln(1+x) \approx x$) and does not cause non-linearity (k_c and k_d = constant) in chemistry, ΔO_3 is linearly proportional to $\Delta v_d/v_d$. The error of linearizing the natural logarithms equals to the difference between $\ln(1+x)$ and x. This analysis gives the conditions for when the first-order approximation is reasonable, and allowing us to estimate the error when deviating from these condition. Assuming β is correctly estimated by chemical transport model, the error of linearization at $\Delta v_d/v_d = \pm 50\%$ (the upper bound of $\Delta v_d/v_d$ consistent with our analysis), is on the order of 25%. For more typical value of $\Delta v_d/v_d$ (20%), the error is around 10%.

As $\Delta v_d/v_d$ gets larger, we can expand R.H.S of S3 to the second order and investigate sensitivity of ΔO_3 to $\Delta v_d/v_d$:

$$\Delta O_3 = \beta \frac{\Delta v_d}{v_d} - \frac{\beta^2}{2O_3}\left(\frac{\Delta v_d}{v_d}\right)^2 = \left(\beta - \frac{\beta^2}{2O_3}\frac{\Delta v_d}{v_d}\right)\left(\frac{\Delta v_d}{v_d}\right) = \beta' \frac{\Delta v_d}{v_d} \ (S6)$$

Where β' is the "corrected β", which is a function of $\Delta v_d/v_d$.

To illustrate the potential impact of such non-linearity on ΔO_3, we compare July $\Delta O_{3,Z03\_BB}$ estimated using first-order estimation with β derived from $\Delta v_d/v_d = +15\%$ (fig. S1b) and +30% (fig. S1a), and second-order approximation (fig. S1c), and the result is shown in figure S1. The three different methods produce very similar ΔO_3, and their differences have little impact on our conclusion. For simplicity, we only show the result using β derived from $\Delta v_d/v_d = +30\%$ in the main manuscript.

As noted above and in the main manuscript, our approach is limited by the assumption that chemistry and transport do not introduce non-linear terms which may not be realistic. Rather, our approach is intended to identify hotspots of impact, and quantify these potential impacts to a first order. More rigorous modeling efforts could then be targeted in future work.

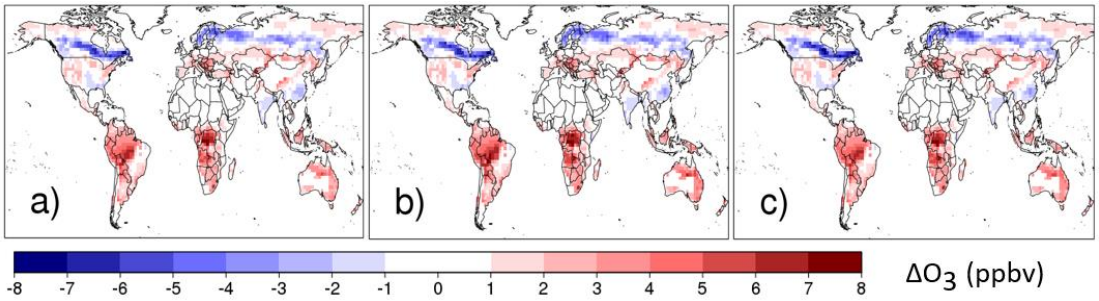

Figure S1. July $\Delta O_{3,Z03\_BB}$ calculated using a) first-order method where β is derived from $\Delta v_d/v_d$ = +30% GC sensitivity run, b) first order method where β is derived from $\Delta v_d/v_d$ = +15% GC sensitivity run, and c) second-order method with β derived from $\Delta v_d/v_d$ = +15%.

2. A brief description of photosynthesis-stomatal conductance (A_n-g_s) module in TEMIR (a manuscript is in prep)

TEMIR largely follows Oleson et al. (2013), where net photosynthetic rate (A_n, μmol CO_2 m^{-2} s^{-1}), stomatal conductance for water (g_{sw}, μmol m^{-2} s^{-1}) and CO_2 concentration in leaf mesophyll (c_i, mol mol^{-1}) are solved simultaneously by the following coupled set of equations:

$$A_n = \frac{g_{sw}}{1.6}(c_a - c_i)\ (S7)$$

$$g_{sw} = \beta_t g_0 + g_1 \frac{A_n}{c_s} RH_s\ (S8)$$

$$A_n = A - R_d\ (S9)$$

Here, c_a is CO_2 concentration (mol mol^{-1}), β_t is soil moisture stress factor (unitless), g_0 is minimum stomatal conductance (μmol m^{-2} s^{-1}), A_n is net photosynthetic rate (μmol CO_2 m^{-2} s^{-1}), A is gross photosynthetic rate (μmol CO_2 m^{-2} s^{-1}) and R_d is dark respiration rate (μmol CO_2 m^{-2} s^{-1}). Furthermore, c_s and RH_s are the CO_2 concentration (mol mol^{-1}) and relative humidity (unitless) at leaf surface. A is calculated following Bonan et al. (2011), which is based on Farquhar et al. (1980) and Collatz et al. (1992):

$$\Theta_{cj} A_i^2 - (A_c + A_j) A_i + A_c A_j = 0\ (S10)$$

$$\Theta_{ip} A^2 - (A_i + A_p) A + A_i A_p = 0\ (S11)$$

For C3 plants, Θ_{cj} = 0.98 and Θ_{ip} = 0.95. For C4 plants, Θ_{cj} = 0.80 and Θ_{ip} = 0.95. Rubisco-limited rate (A_c, μmol CO_2 m^{-2} s^{-1}), light-limited rate (A_j, μmol CO_2 m^{-2} s^{-1}), product-limited rate (A_p, μmol CO_2 m^{-2} s^{-1}) and R_d are calculated as:

$$A_c = \begin{cases} \dfrac{V_{c\,max}(c_i - \Gamma_*)}{c_i + K_c(1 + \dfrac{0.21P_{atm}}{K_o})} \; for\; C_3\; plants \\ V_{c\,max} \;\; for\; C_4\; plants \end{cases} \quad (S12)$$

$$A_j = \begin{cases} \dfrac{J(c_i - \Gamma_*)}{4c_i + 8\Gamma_*} \; for\; C_3\; plants \\ 0.23\phi \;\; for\; C_4\; plants \end{cases} \quad (S13)$$

$$A_c = \begin{cases} 3T_p \; for\; C_3\; plants \\ k_p \dfrac{c_i}{P_{atm}} \;\; for\; C_4\; plants \end{cases} \quad (S14)$$

$$R_d = \begin{cases} 0.015V_{c\,max} \; for\; C_3\; plants \\ 0.025V_{c\,max} \;\; for\; C_4\; plants \end{cases} \quad (S15)$$

Here, V_{cmax}, Γ_*, P_{atm}, J, φ, T_p and k_p are the maximum rate of carboxylation (μmol m^{-2} s^{-1}), CO_2 compensation point (mol mol^{-1}), atmospheric pressure (Pa), electron transport rate (μmol m^{-2} s^{-1}), absorbed photosynthetically active radiation (PAR) (W m^{-2}), triose phosphate utilization rate (μmol m^{-2} s^{-1}) and initial slope of C_4 CO_2 response curve (μmol Pa^{-1} m^{-2} s^{-1}). K_c and K_o are the Michaelis-Menten constants for CO_2 and O_2 (Pa). Furthermore, J is calculated as the smaller root of the following equation:

$$0.7J^2 + (1.955\phi + J_{max})J + 1.955\phi = 0 \; (S16)$$

Where J_{max} is the maximum potential rate of electron transport (μmol m^{-2} s^{-1}). As J_{max}, φ, V_{cmax} and the variables related to V_{cmax} (Γ_*, J_{max}, T_p, R_d) differ between sunlit and shaded leaves, the above set of equations are solved separately for sunlit and shaded leaves.

The parameters (V_{cmax}, Γ_*, K_c, K_o, J_{max}, T_p, R_d) are functions of vegetation temperature (T_v), and the temperature scaling formulae are given at eq. 8.9 to eq. 8.14, while the effect of temperature acclimation (Kattge and Knorr, 2007) on J_{max} and V_{cmax} are given at eq. 8.15 and 8.16 in Oleson et al. (2013). Other details of the model formalism (e.g. canopy scaling and effect of β_t on V_{cmax}) also follow Chapter 8 in Oleson et al. (2013), therefore we will focus on describing the main differences between CLM 4.5 and TEMIR.

First, TEMIR is driven entirely by assimilated meteorology. Instead of solving the whole surface energy balance equation, TEMIR consistently calculates T_v from 2-meter air temperature (T_2, K) and sensible heat flux (H, W m^{-2}) using Monin-Obukhov similarity theory (Monin and Obukhov, 1954):

$$T_v = T_2 + \frac{H}{\rho c_p}(r_{a,h} + r_{b,h}) \; (S16)$$

Where ρ, c_p, $r_{a,h}$ and $r_{b,h}$ are air density (kg m^{-3}), specific heat of air at constant pressure (J kg^{-1} K^{-1}), aerodynamic and laminar boundary-layer resistance (s m^{-1}) of heat, respectively.

Secondly, MERRA-2 only provides soil moisture output at two levels (surface and root zone), which is not compatible with the multi-layer soil module in CLM. Therefore, instead of aggregating β_t from multiple soil layers, TEMIR calculates β_t from the root-zone soil wetness of MERRA-2. Soil wetness (s) is first converted into soil matric potential (ψ, mm) using the following equation:

$$\psi = \psi_{sat} s^{-B} \; (S17)$$

Where ψ_{sat} and B are the soil matric potential (mm) at saturation and Clapp-Hornberger exponent (Clapp and Hornberger, 1978), which are related to soil property. Then β_t is calculated as:

$$\beta_t = \frac{\psi_c - \psi}{\psi_c - \psi_0}\left(\frac{\theta_{sat} - \theta_{ice}}{\theta_{sat}}\right), 0 \le \beta_t \le 1 \ (S18)$$

Where ψ_c and ψ_0 are the soil matric potential (mm) at which stomata are full close or fully open, and the term in the bracket account for the fact that frozen water are not available for plants.

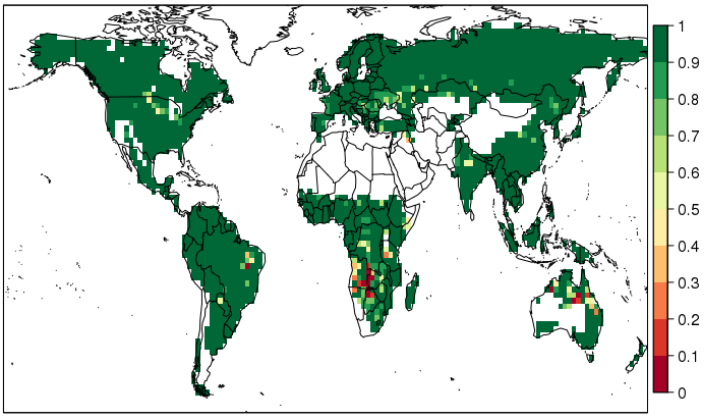

Figure S2. July average soil moisture stress factor (β_t). β_t = 1 represents no soil moisture stress, while smaller β_t means stronger soil moisture stress and more stomatal closure. β_t = 0 signifies that soil moisture stress is so strong that it completely shuts down stomatal activity.

3. Table S1 to Table S3

	W98	Z03	W98_BB	Z03_BB
R_a	$R_a = \frac{1}{\kappa u_*}\left[\ln(\frac{z}{z_0}) - \Psi\left(\frac{z}{L}\right) + \Psi(\frac{z_0}{L})\right]$ When $\varsigma \geq 0, \Psi(\varsigma) = -5\varsigma$ When $\varsigma < 0, \Psi(\varsigma) = 2\ln(\frac{1+\sqrt{1-16\varsigma}}{2})$			
R_b	$R_b = \frac{2}{\kappa u_*}(\frac{Sc}{Pr})^{2/3}$			
R_s	$R_s = r_s(PAR, LAI) f_T \frac{D_{\mathrm{H_2O}}}{D_{\mathrm{O_3}}}$	$R_s = \frac{r_s(PAR, LAI)}{(1-w_{st}) f_T f_{vpd} f_\psi} \frac{D_{\mathrm{H_2O}}}{D_{\mathrm{O_3}}}$	$g_s = g_0 + m\frac{A_n}{C_s}h_s$ $R_s = \frac{1}{g_s}\frac{D_{\mathrm{H_2O}}}{D_{\mathrm{O_3}}}$	$g_s = g_0 + m\frac{A_n}{C_s}h_s$ $R_s = \frac{1}{(1-w_{st})g_s}\frac{D_{\mathrm{H_2O}}}{D_{\mathrm{O_3}}}$
Cuticular Resistance (R_{cut})	$R_{cut} = \frac{R_{cut_0}}{LAI}$	For dry surface, $R_{cut} = \frac{R_{cut_{d0}}}{e^{0.03RH} LAI^{0.25} u_*}$ For wet surface, $R_{cut} = \frac{R_{cut_{w0}}}{LAI^{0.5} u_*}$	Same as W98	Same as Z03
In-canopy aerodynamic resistance (R_{ac})	Prescribed	$R_{ac} = R_{ac_0}\frac{LAI^{0.25}}{u_*}$		
Ground Resistance (R_g)	Prescribed			
Lower-canopy aerodynamic resistance (R_{alc})	$R_{alc} = 100(1 + \frac{1000}{R+10})$	-		
Lower-canopy surface resistance (R_{clc})	Prescribed	-		

Table S1: Brief description of the four dry deposition parameterizations. κ = von Karman constant, u_* = friction velocity, z = reference height, z_0 = roughness length, L = Obukhov length, Sc = Schmidt's number, Pr = Prandtl number for air, LAI = leaf area index, PAR = photosynthetically active radiation, D_x = Diffusivity of species x in air, f_T = temperature (T) stress function, f_{vpd} = vapour pressure deficit (VPD) stress function, f_ψ = leaf water potential (ψ) stress function, w_{st} = stomatal blocking fraction, A_n = Net photosynthetic rate, g_0 = minimum stomatal conductance, m = Ball-Berry slope, C_s = CO_2 concentration on leaf surface, h_s = relative humidity on leaf surface, RH = relative humidity, h = canopy height, R = downward shortwave radiation

CLM PFT	Z03 surface type
Needleleaf evergreen tree - temperate	Evergreen needleleaf trees
Needleleaf evergreen tree - boreal	
Needleleaf deciduous tree - boreal	Deciduous needleleaf trees
Broadleaf evergreen tree - tropical	Tropical broadleaf trees
Broadleaf deciduous tree - tropical	Deciduous broadleaf trees
Broadleaf deciduous tree - temperate	
Broadleaf deciduous tree - boreal	
Broadleaf evergreen shrub - temperate	Thorn shrubs
Broadleaf deciduous shrub - temperate	Deciduous shrubs
Broadleaf deciduous shrub - boreal	
C_3 arctic grass	Tundra
C_3 grass	Short grass
C_4 grass	Corn*
C_3 crop	Crops

Table S2: Mapping between CLM PFT and Z03 surface type.

*C_4 grasses are mapped to corn due to the similarity in photosynthetic pathway, and hence stomatal control

Land Type	Longitude	Latitude	Season	Mean daytime v_d (cm s^{-1})	Citation
Deciduous Forest	-80.9°	44.3°	Summer	0.92	Padro et al., 1991
			Winter	0.28	
	99.7°	18.3°	Spring	0.38	Matsuda et al., 2005
			Summer	0.65	
	-72.2°	42.7°	Summer	0.61	Munger et al., 1996
			Winter	0.28	
	-78.8°	41.6°	Summer	0.83	Finkelstein et al., 2000
	-75.2°	43.6°	Summer	0.82	
Coniferous Forest	-3.4°	55.3°	Spring	0.58	Coe et al., 1995
	-79.1°	36.0°	Spring	0.79	Finkelstein et al., 2000
	-120.6°	38.9°	Spring	0.58	Kurpius et al., 2002
			Summer	0.59	
			Autumn	0.43	
			Winter	0.45	
	-0.7°	44.2°	Summer	0.48	Lamaud et al., 1994
	105.5°	40.0°	Summer	0.39	Turnipseed et al., 2009
	-66.7°	54.8°	Summer	0.26	Munger et al., 1996
	11.1°	60.4°	Spring	0.31	Hole et al., 2004
			Summer	0.48	
			Autumn	0.20	
			Winter	0.074	
	8.4°	56.3°	Spring	0.68	Mikkelsen et al., 2004
			Summer	0.80	
			Autumn	0.83	
Tropical Rainforest	117.9°	4.9°	Wet	0.5	Fowler et al., 2011#
			Wet	1.0	
	-61.8°	-10.1°	Wet	1.1	Rummel et al., 2007
			Dry	0.5	
	-60.0°	3.0°	Wet	1.8	Song-Miao et al., 1990
Grass	-88.2°	40.0°	Summer	0.56	Droppo, 1985

	-3.2°	57.8°	Spring	0.59	Fowler et al., 2001
			Summer	0.56	
			Autumn	0.42	
	-119.8°	37.0°	Summer	0.15	Padro et al., 1994
	-8.6°	40.7°	Summer	0.22	Pio et al., 2000
			Winter	0.38	
	-104.8°	40.5°	Spring	0.22	Stocker et al., 1993
	10.5°	52.4°	Spring	0.44	Meszáros et al., 2009
	-96.4°	39.5°	Summer	0.62	Gao and Wesely, 1995
Crops	-2.8°	55.9°	Not applicable*	0.69	Coyle et al., 2009
	-88.4°	40.1°		0.53	Meyers et al., 1998
				0.12	
	-87.0°	36.7°		0.85	
				0.39	
	-86.0°	34.3°		0.40	
	-120.7°	36.8°		0.76	Padro et al., 1994
	8.0°	48.7°		0.41	Pilegaard et al., 1998
	2.0°	48.9°		0.60	Stella et al., 2011
	0.6°	44.4°		0.47	
	1.4°	43.8°		0.37	

Table S3: Information on all the measurement sites included in model evaluation

*Crops are heavily influenced by management practices rather than natural seasonality. Thus, two data sets in the same location generally represent before and after certain a crop phenology or human management event.

[#]The two measurements are taken at a rainforest and an oil palm plantation nearby.

4. References

Bonan, G. B., Lawrence, P. J., Oleson, K. W., Levis, S., Jung, M., Reichstein, M., Lawrence, D. M. and Swenson, S. C.: Improving canopy processes in the Community Land Model version 4 (CLM4) using global flux fields empirically inferred from FLUXNET data, J. Geophys. Res., 116(G2), G02014, doi:10.1029/2010jg001593, 2011.

Clapp, R. B. and Hornberger, G. M.: Empirical equations for some soil hydraulic properties, Water Resour. Res., 14(4), 601–604, doi:10.1029/WR014i004p00601, 1978.

Coe, H., Gallagher, M. W., Choularton, T. W. and Dore, C.: Canopy scale measurements of stomatal and cuticular 03 uptake by sitka spruce, Atmos. Environ., 29(12), 1413–1423, doi:10.1016/1352-2310(95)00034-V, 1995.

Collatz, G., Ribas-Carbo, M. and Berry, J.: Coupled Photosynthesis-Stomatal Conductance Model for Leaves of C4 Plants, Funct. Plant Biol., 19(5), 519, doi:10.1071/pp9920519, 1992.

Coyle, M., Nemitz, E., Storeton-West, R., Fowler, D. and Cape, J. N.: Measurements of ozone deposition to a potato canopy, Agric. For. Meteorol., 149(3–4), 655–666, doi:10.1016/j.agrformet.2008.10.020, 2009.

Droppo, J. G.: Concurrent measurements of ozone dry deposition using eddy correlation and profile flux

methods., J. Geophys. Res., 90(D1), 2111–2118, doi:10.1029/JD090iD01p02111, 1985.

Farquhar, G. D., von Caemmerer, S. and Berry, J. A.: A biochemical model of photosynthetic CO2 assimilation in leaves of C3 species, Planta, 149(1), 78–90, doi:10.1007/BF00386231, 1980.

Finkelstein, P. L., Ellestad, T. G., Clarke, J. F., Meyers, T. P., Schwede, D. B., Hebert, E. O. and Neal, J. A.: Ozone and sulfur dioxide dry deposition to forests: Observations and model evaluation, J. Geophys. Res. Atmos., 105(D12), 15365–15377, doi:10.1029/2000JD900185, 2000.

Fowler, D., Flechard, C., Cape, J. N., Storeton-West, R. L. and Coyle, M.: Measurements of ozone deposition to vegetation quantifying the flux, the stomatal and non-stomatal components, Water. Air. Soil Pollut., 130(1–4), 63–74, doi:10.1023/A:1012243317471, 2001.

Fowler, D., Nemitz, E., Misztal, P., di Marco, C., Skiba, U., Ryder, J., Helfter, C., Neil Cape, J., Owen, S., Dorsey, J., Gallagher, M. W., Coyle, M., Phillips, G., Davison, B., Langford, B., MacKenzie, R., Muller, J., Siong, J., Dari-Salisburgo, C., di Carlo, P., Aruffo, E., Giammaria, F., Pyle, J. A. and Nicholas Hewitt, C.: Effects of land use on surface-atmosphere exchanges of trace gases and energy in Borneo: Comparing fluxes over oil palm plantations and a rainforest, Philos. Trans. R. Soc. B Biol. Sci., 366(1582), 3196–3209, doi:10.1098/rstb.2011.0055, 2011.

Gao, W. and Wesely, M. L.: Modeling gaseous dry deposition over regional scales with satellite observations-I. Model development, Atmos. Environ., 29(6), 727–737, doi:10.1016/1352-2310(94)00284-R, 1995.

Hole, L. R., Semb, A. and Tørseth, K.: Ozone deposition to a temperate coniferous forest in Norway; gradient method measurements and comparison with the EMEP deposition module, in Atmospheric Environment, vol. 38, pp. 2217–2223., 2004.

Kattge, J. and Knorr, W.: Temperature acclimation in a biochemical model of photosynthesis: A reanalysis of data from 36 species, Plant, Cell Environ., 30(9), 1176–1190, doi:10.1111/j.1365-3040.2007.01690.x, 2007.

Kurpius, M. R., McKay, M. and Goldstein, A. H.: Annual ozone deposition to a Sierra Nevada ponderosa pine plantation, Atmos. Environ., 36(28), 4503–4515, doi:10.1016/S1352-2310(02)00423-5, 2002.

Lamaud, E., Brunet, Y., Labatut, A., Lopez, A., Fontan, J. and Druilhet, A.: The Landes experiment: biosphere-atmosphere exchanges of ozone and aerosol particles above a pine forest, J. Geophys. Res., 99(D8), doi:10.1029/94jd00668, 1994.

Matsuda, K., Watanabe, I., Wingpud, V., Theramongkol, P., Khummongkol, P., Wangwongwatana, S. and Totsuka, T.: Ozone dry deposition above a tropical forest in the dry season in northern Thailand, Atmos. Environ., 39(14), 2571–2577, doi:10.1016/j.atmosenv.2005.01.011, 2005.

Mészáros, R., Horváth, L., Weidinger, T., Neftel, A., Nemitz, E., Dämmgen, U., Cellier, P. and Loubet, B.: Measurement and modelling ozone fluxes over a cut and fertilized grassland, Biogeosciences Discuss., 6(1), 1069–1089, doi:10.5194/bgd-6-1069-2009, 2009.

Meyers, T. P., Finkelstein, P., Clarke, J., Ellestad, T. G. and Sims, P. F.: A multilayer model for inferring dry deposition using standard meteorological measurements, J. Geophys. Res. Atmos., 103(D17), 22645–22661, doi:10.1029/98JD01564, 1998.

Mikkelsen, T. N., Ro-Poulsen, H., Hovmand, M. F., Jensen, N. O., Pilegaard, K. and Egeløv, A. H.: Five-year measurements of ozone fluxes to a Danish Norway spruce canopy, in Atmospheric Environment, vol. 38, pp. 2361–2371., 2004.

Monin, A. S. and Obukhov, A. M.: Basic laws of turbulent mixing in the surface layer of the atmosphere,

Contrib. Geophys. Inst. Acad. Sci. USSR, 24(151), 163–187, 1954.

Munger, W. J.: Atmospheric deposition of reactive nitrogen oxides and ozone in a temperate deciduous forest and a subarctic woodland 1. Measurements and mechanisms, J. Geophys. Res. Atmos., 101(D7), 12639–12657, doi:10.1029/96jd00230, 1996.

Oleson, K. W., Lawrence, D. M., Bonan, G. B., Drewniak, B., Huang, M., Koven, C. D., Levis, S., Li, F., Riley, W. J., Subin, Z. M., Swenson, S. C., Thornton, P. E., Bozbiyik, A., Fisher, R., Heald, C. L., Kluzek, E., Lamarque, J.-F., Lawrence, P. J., Leung, L. R., Lipscomb, W., Muszala, S., Ricciuto, D. M., Sacks, W., Sun, Y., Tang, J. and Yang, Z.-L.: Technical Description of version 4.5 of the Community Land Model (CLM), NCAR/TN-478+STR NCAR Tech. Note, (April), NCAR/TN-503+STR, doi:10.5065/D6RR1W7M, 2013.

Padro, J., den Hartog, G. and Neumann, H. H.: An investigation of the ADOM dry deposition module using summertime O3 measurements above a deciduous forest, Atmos. Environ. Part A, Gen. Top., 25(8), 1689–1704, doi:10.1016/0960-1686(91)90027-5, 1991.

Padro, J., Massman, W. J., Shaw, R. H., Delany, A. and Oncley, S. P.: A comparison of some aerodynamic resistance methods using measurements over cotton and grass from the 1991 California ozone deposition experiment, Boundary-Layer Meteorol., 71(4), 327–339, doi:10.1007/BF00712174, 1994.

Pilegaard, K., Hummelshøj, P. and Jensen, N. O.: Fluxes of ozone and nitrogen dioxide measured by eddy correlation over a harvested wheat field, Atmos. Environ., 32(7), 1167–1177, doi:10.1016/S1352-2310(97)00194-5, 1998.

Pio, C. A., Feliciano, M. S., Vermeulen, A. T. and Sousa, E. C.: Seasonal variability of ozone dry deposition under southern European climate conditions, in Portugal, Atmos. Environ., 34(2), 195–205, doi:10.1016/S1352-2310(99)00276-9, 2000.

Rummel, U., Ammann, C., Kirkman, G. A., Moura, M. A. L., Foken, T., Andreae, M. O. and Meixner, F. X.: Seasonal variation of ozone deposition to a tropical rain forest in southwest Amazonia, Atmos. Chem. Phys., 7(20), 5415–5435, doi:10.5194/acp-7-5415-2007, 2007.

Song-Miao Fan, Wofsy, S. C., Bakwin, P. S., Jacob, D. J. and Fitzjarrald, D. R.: Atmosphere-biosphere exchange of CO2 and O3 in the central Amazon forest, J. Geophys. Res., 95(D10), doi:10.1029/jd095id10p16851, 1990.

Stella, P., Personne, E., Loubet, B., Lamaud, E., Ceschia, E., Béziat, P., Bonnefond, J. M., Irvine, M., Keravec, P., Mascher, N. and Cellier, P.: Predicting and partitioning ozone fluxes to maize crops from sowing to harvest: The Surfatm-O 3 model, Biogeosciences, 8(10), 2869–2886, doi:10.5194/bg-8-2869-2011, 2011.

Stocker, D. W., Stedman, D. H., Zeller, K. F., Massman, W. J. and Fox, D. G.: Fluxes of nitrogen oxides and ozone measured by eddy correlation over a shortgrass prairie, J. Geophys. Res., 98(D7), doi:10.1029/93jd00871, 1993.

Turnipseed, A. A., Burns, S. P., Moore, D. J. P., Hu, J., Guenther, A. B. and Monson, R. K.: Controls over ozone deposition to a high elevation subalpine forest, Agric. For. Meteorol., 149(9), 1447–1459, doi:10.1016/j.agrformet.2009.04.001, 2009.